The uncertainties in the cross sections over the 1.07 Mev resonance at 125.2°, 131.2°, 140.7°, 149.5°, and 167.7° have not been included in Table I(a) because of a possible systematic error in these data. These data were taken with a 1000-A counter foil whose copper backing had not been completely and uniformly removed. No other data were taken with this foil. Comparison data at 109.9° taken with a completely copper-stripped foil indicated that 9 percent of the foil area was opaque to the scattered deuterons. This correction has been applied to the data at the five angles and the energies mentioned above. It is possible that these corrections should be more than 9 percent because the scattered deuteron energies are lower at these angles than at 109.9° and less copper is required to stop the deuterons. The deuteron energies at which the resonance peaks occur are not affected by this error.

The cylindrical analyzer was calibrated in terms of the $Li^7(p,n)Be^7$ threshold (assumed equal to 1.8816 Mev±0.05 percent[12]). Corrections were applied for the loss of energy in the helium between the cylindrical analyzer and the center of the scattering chamber, for beam-induced current on the analyzer plates, and for the relativistic mass increase. On the 1.07-Mev resonance the total correction varied from 3 to 6 kev.

[12] F. Ajzenberg and T. Lauritsen, Revs. Modern Phys. **24**, 321 (1952), bottom of p. 334.

Because of interference effects, the deuteron energy for the peak yield should be different at different angles. In fact the variation is a sensitive test for the phase shift analysis of the accompanying paper.[7] Table II lists for the 1.07-Mev resonance the energies for the peak cross sections at various angles. (At 90° where no peak occurs the energy of the dip is given.)

V. COMPARISON WITH OTHER CROSS-SECTION MEASUREMENTS

In a recent experiment performed by Lauritsen, Huus, and Nilsson[2] the deuteron-helium differential cross sections were measured to 10–20 percent accuracy at 90°, 120°, and 156° c.m. from $E_d=1.0$ to 1.2 Mev. Their 90° data agree with ours to within their experimental errors. Plots of the cross sections as functions of angle show a similar agreement for their 120° and 156° data.

The solid points in Fig. 3 are interpolated from the data of Blair *et al.*[13] They are in agreement with the open points, which were obtained in the present experiment. The uncertainties in Blair's data are about 3 percent.

An interpretation of these cross sections in terms of parameters of the energy states of Li^6 is given in an accompanying paper.[7]

[13] Blair, Freier, Lampi, and Sleator, Phys. Rev. **75**, 1678 (1949).

PHYSICAL REVIEW VOLUME 98, NUMBER 3 MAY 1, 1955

Energy Levels of Li^6 from the Deuteron-Helium Differential Cross Sections*

A. GALONSKY† AND M. T. MCELLISTREM
University of Wisconsin, Madison, Wisconsin
(Received December 27, 1954)

The deuteron-helium differential cross sections presented in the preceding paper have been analyzed in terms of a dispersion formalism to classify energy levels of Li^6. A level at $E_x=2.185$ Mev is confirmed to be a single particle, 3^+, $T=0$ level. The broad anomaly extending from 3 Mev to the limit of observation, 4.62 Mev, cannot be analyzed in terms of a single level. Instead, it has been fitted with two single-particle levels, a 2^+ level at $E_x=4.53$ Mev in Li^6 and a 1^+ level at 5.4±0.5 Mev. The 1^+ level cannot be located more accurately because only the tail is visible at the bombarding energies available. All of the other two-level combinations have been ruled out. The assignments, (3^+, 2^+, 1^+), and locations of the levels agree with an intermediate coupling model which is close to the $L-S$ extreme. In the neighborhood of and above the 3^+ resonance the usual hard-sphere phase shifts, which are always negative, cannot be used for the P-wave. This result may indicate odd-parity states above the presently investigated energy region. For the other partial waves, hard-sphere phase shifts corresponding to radii anywhere from 3 to 5×10^{-13} cm were satisfactory, provided the reduced width of the ground state of Li^6 was simultaneously varied from the Wigner limit to very small values.

I. INTRODUCTION

THE differential cross sections presented in the preceding paper are empirical facts of the deuteron-helium system for which a nuclear theory must account. It is, however, possible to meet the theory part-way by fitting the cross sections with a small number of parameters. These parameters should then be significant numbers to be derived by any specific nuclear theory. Reaction cross sections can always be described in terms of parameters of quasi-stationary states of the compound nucleus, such as angular momenta, parities, resonance energies, and level widths.[1,2]

* Work supported by the U. S. Atomic Energy Commission and the Wisconsin Alumni Research Foundation.
† Now at Oak Ridge National Laboratory, Oak Ridge, Tennessee.

[1] E. P. Wigner and L. Eisenbud, Phys. Rev. **72**, 29 (1947).
[2] T. Teichmann and E. P. Wigner, Phys. Rev. **87**, 123 (1952)

As the total number of levels is infinite, the dispersion formalism is of practical use only if the cross section can be represented in terms of a few neighboring levels plus a slowly varying contribution from all distant levels. This latter contribution can be represented by an additional parameter, the interaction distance, which must be approximately the sum of the radii of the interacting particles. The dispersion formalism in this "one-level" approximation and as applied to measured cross sections gives definite values for the angular momenta, parities, and resonance energies of the compound states; the reduced widths and interaction distances are less uniquely determined.

In Li^6 one may expect to find ten states just from the coupling of the two p-shell nucleons. The coupling of these nucleons might be expected to be a dominant factor for some of the first few states, since the alpha-particle core has no low-lying excited states. The present data will be shown to support this view and to shed light on the nature of the coupling at low excitation.

II. KINEMATICS OF THE SCATTERING PROCESS

In Appendix I, the general partial wave expansion is specialized for the case of elastic scattering of spin-one by spin-zero particles.

The result of the expansion in Appendix I is that the differential cross section is of the form

$$3k^2\frac{d\sigma}{d\Omega}=2|A|^2+|B|^2+\sin^2\theta\{|C|^2+|D|^2\}+\sin^4\theta\{|E|^2\},$$

where $k=\mu v/\hbar$ and θ is the c.m. scattering angle. A and B arise from scatterings with no change of spin magnetic quantum number, m_s, and therefore involve interference with Rutherford scattering amplitudes; C and D come from m_s changing by ±1 and E corresponds to m_s changing by ±2. Hence no interference with Coulomb scattering is included in terms of C, D, and E.

Most of the complexity of the resulting formula (Appendix I) is due to the "large" channel spin S. Because $S=1$ it is possible to excite a given J by two l-values and still conserve parity. On a 3^+ resonance, for example, there are four possible situations: D-waves coming in and going out; G-waves in and out; D-waves in, G-waves out; and G-waves in, D-waves out.

The $\sin\theta$ factors multiplying C, D, and E provide a great simplification for scattering angles near 180° where $\sin\theta\to0$. This result is made plausible if it is remembered that $\mathbf{l}$ is perpendicular to the beam axis for a particle either ingoing or outgoing along that axis. Thus, for 180° scattering, $m_l=0$ and $m_s=m_{s'}$.

III. SINGLE-LEVEL APPROXIMATION

The quantities A, B, C, D, and E (see Appendix I) involve vector sums of Coulomb amplitude and/or amplitudes from all partial waves. The Coulomb amplitudes and angles are, of course, well known; all coefficients of the partial wave amplitudes are also well known (e.g., Legendre polynomials and derivatives) except for the elements $U_{ll'}{}^J$ of the collision matrix. All the nuclear physics is buried in the collision matrix. The measured cross sections must, therefore, be used to determine the $U_{ll'}{}^J$, or what is equivalent, the phase shifts of the various partial waves. This phase shift analysis may be done empirically with the aid of modern computing machines. For example, Haeberli and Galonsky have used the method of Fermi and Metropolis[3] to analyze some proton-neon cross-section data.[4] The computing machine available, an IBM-CPC Model I, was so slow and the scattering formula of Appendix I so complicated that the method was abandoned for the deuteron-helium work. Instead, the simplifications that arise from the dispersion formalism were put in from the start of the analysis.

According to the single-level approximation[1,2] the elements, $U_{ll'}{}^J$, of the collision matrix are[5,6]:

$$U_{l,l}{}^{l}=\exp[2i(\phi_l+\beta^l)],\quad (J=l)$$

$$U_{l,l}{}^{l\pm1}=e^{2i\phi_l}\left(\frac{\Gamma_{\lambda,l\pm2}}{\Gamma_\lambda}+\frac{\Gamma_{\lambda,l}}{\Gamma_\lambda}\exp(2i\beta^{l\pm1})\right),\quad (J=l\pm1)$$

$$U_{l\pm2,l}{}^{l\pm1}=U_{l,l\pm2}{}^{l\pm1}=\pm e^{i(\phi_l+\phi_{l\pm2})}\frac{(\Gamma_{\lambda,l}\Gamma_{\lambda,l\pm2})^{\frac{1}{2}}}{\Gamma_\lambda}\times2i\sin\beta^{l\pm1}\exp(i\beta^{l\pm1}),\quad (J=l\pm1)$$

where

$$\tan\beta^J=\frac{\Gamma_\lambda/2}{E_R-E},\quad \left(\begin{matrix}\Gamma_\lambda=\Gamma_{\lambda,l}\text{ for }J=l\\ \Gamma_\lambda=\Gamma_{\lambda,l}+\Gamma_{\lambda,l\pm2}\text{ for }J=l\pm1\end{matrix}\right),$$

$$\frac{\Gamma_{\lambda,l}}{2}=\frac{k\gamma_{\lambda,l}{}^2}{A_l{}^2},$$

$$E_R=E_\lambda+\Delta_\lambda,$$

$$\left\{\begin{matrix}\Delta_\lambda=\dfrac{-\gamma_{\lambda,l}{}^2}{a}[g_l+l]\text{ for }J=l\\ \Delta_\lambda=\dfrac{-\gamma_{\lambda,l}{}^2}{a}[g_l+l]-\dfrac{\gamma_{\lambda,l\pm2}{}^2}{a}[g_{l\pm2}+l\pm2]\text{ for }J=l\pm1\end{matrix}\right\},$$

$$g_l=\frac{d(\ln A_l)}{d(\ln(ka))}$$

and $\tan\phi_l=-(F_l/G_l)_a$.

[3] Fermi, Metropolis, and Alei, Phys. Rev. **95**, 1581 (1954).

[4] Haeberli, Douglas, Galonsky, and Goldberg, Phys. Rev. **91**, 438(A) (1953).

[5] R. G. Sachs, *Nuclear Theory* (Addison-Wesley Press, Cambridge, 1953), pp. 300 ff.

[6] It is assumed that elastic scattering is the only reaction occurring so that the total width, Γ_λ, is the elastic scattering width. Capture with the subsequent emission of a γ ray is always energetically possible, but the electromagnetic interaction is so much weaker than the nuclear interaction that this process can well be neglected. The binding energy of the deuteron is such that the $He^4(d,p\gamma)He^4$ reaction is possible for deuteron bombarding energies above 3.346 Mev. The cross section is expected to be low near threshold. J. C. Allred *et al.*, Phys. Rev. **82**, 786 (1951) find the total cross section at 10.3 Mev to be 30 percent of the elastic cross section. In the present experiment the reaction would not have been observed because of the low proton energies possible in the energy range investigated. At 4.2-Mev deuteron energy the maximum proton energy is only 0.12 Mev at 90° Lab.

The parameters E_λ, $\gamma_{\lambda,l}^2$, and a are to be determined by fitting the experimental cross sections. E_λ is the characteristic energy of the state X_λ of the compound nucleus, Li^6 in this case. Because the value of E_λ depends both upon a somewhat arbitrary boundary condition, and upon the interaction distance a, E_R is taken as the more significant parameter.

$\gamma_{\lambda,l}^2$ is the reduced width of X_λ leading to the decay of the Li^6 state into a deuteron and an α particle with relative orbital angular momentum, l. $\Gamma_{\lambda,l}$, which is proportional to the probability for this decay, is the product of the purely nuclear probability, $\gamma_{\lambda,l}^2$, with an inhibiting Coulomb and centrifugal barrier factor, $1/A_l^2$,[7] and a momentum factor, k. Clearly it is $\gamma_{\lambda,l}^2$ rather than $\Gamma_{\lambda,l}$ which is the more fundamental quantity for nuclear theory. A consequence of the single-level approximation is that the net effect on the cross section of the infinitude of distant levels can be represented in the collision matrix as a slowly varying phase shift, ϕ_l, which shall hereafter be referred to as a "potential" phase shift to distinguish it from the $\beta^{J\pi}$, the resonant phase shifts. Although the "potential" phase shifts, ϕ_l, actually express the effect of the other (distant) levels, they cannot be considered as simply the algebraic sum of the very many and very small resonant phase shifts of these levels. Such a sum could give only *positive* phase shifts whereas the approximation listed for ϕ_l (i.e., $\tan\phi_l = -(F_l/G_l)_a$) always gives a negative phase shift and is mathematically equivalent to the phase shifts for scattering by a hard sphere of radius, a.[8] Teichman and Wigner[2] have pointed out that a may vary as a function of l and energy as a consequence of considering specifically only a finite number of the levels of the system. As the number of neighboring levels which are specifically considered is increased one might hope that a fixed a might be a good approximation over quite an energy range. This procedure, which has had rather considerable success in other charged particle experiments,[9] is also used in this analysis.

F_l, G_l, and the quantities derived from them also depend on a. The values of $\gamma_{\lambda,l}^2$ extracted from the data can be quite sensitive to the choice of a through the strong dependence of A_l^2 on a for high l-values and/or low energies.

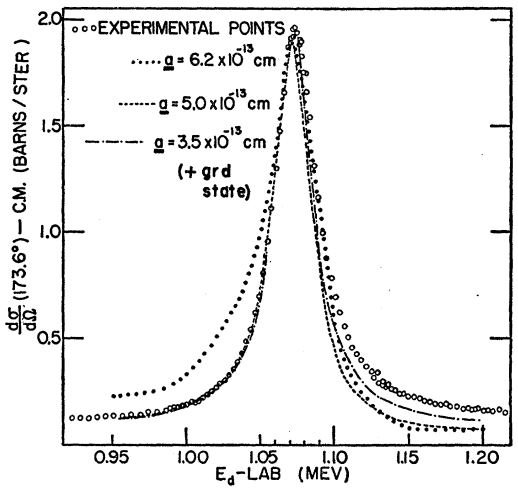

FIG. 1. Deuteron-helium scattering data over 1.07-Mev resonance at 173.6° (c.m.). Curves (dotted, dashed and dot-dashed) are theoretical fits to the data for different assumed distances a. For $a=3.5\times10^{-13}$ cm sufficient ground state resonant S-wave was added to the hard-sphere S-wave to make the resultant S-vector equal to that for hard-sphere alone with $a=5.0\times10^{-13}$ cm.

IV. QUALITATIVE AIDS TO LEVEL CLASSIFICATION

Parity assignments may sometimes be made unambiguously simply from the qualitative behavior of a scattering anomaly.

For example, at energies below E_R by several times the level width, one can assume that the scattering results only from the "potential" phase shifts and Rutherford scattering.[10] Hence $U_{l,l}{}^{l}=U_{l,l}{}^{l\pm1}=U_l$, $U_{l,l-2}{}^{l-1}=U_{l,l+2}{}^{l+1}=0$, and

$$\frac{d\sigma}{d\Omega}=\frac{1}{3k^2}\{2|A|^2+|B|^2\}$$
$$=\frac{1}{k^2}\left|R+\sum_l(2l+1)P_l e^{i\alpha_l}\frac{(U_l-1)}{2i}\right|^2$$

which is a smoothly varying function of energy. As we approach the energy region affected by the resonance, this formula is no longer adequate, and we must return to formula (2) of the Appendix. If the angle of observation is 90° in the c.m. system and a resonance involving odd l occurs, then A and B will continue to vary smoothly over the resonance just as if the resonance

[7] $A_l^2=F_l^2+G_l^2$, where F_l and G_l are the unbound regular and irregular solutions of the Schrödinger equation. A_l^2, g_l, and ϕ_l may be calculated with the aid of Coulomb wave-function tables: I. Bloch *et al.*, Revs. Modern Phys. **23**, 147 (1951) and *Tables of Coulomb Wave Functions*, National Bureau of Standards Applied Mathematics Series (17) (U. S. Government Printing Office, Washington, 1952).

[8] Nowhere in the single-level dispersion formalism is an actual hard sphere potential presumed to exist. However, one can understand why the effect of the distant levels is equivalent to a hard sphere potential by the following considerations. A set of internal wave functions, X_λ, associated with the states of the compound nucleus is a complete set. (Reference 5, p. 291.) At the energy of the isolated resonance the wave function of the reacting particles (in this case the alpha+deuteron wave function) matches at the nuclear surface the X_λ (or linear combination of X_λ's) associated with the resonant state. This particular X_λ is orthogonal to all of the others because of the completeness. The deuteron+alpha function is also orthogonal to them because it matches that particular X_λ. If all the states were distant, the deuteron+alpha function would be orthogonal to all of the internal functions and would, therefore, vanish at the surface. The same vanishing is produced by a hard sphere potential.

[9] p+He—C. L. Critchfield and D. C. Dodder, Phys. Rev. **76**, 602 (1949); p+C^{12}—H. L. Jackson and A. I. Galonsky, Phys. Rev. **89**, 370 (1953); α+C^{12}—R. W. Hill, Phys. Rev. **90**, 845 (1953), and J. Bittner and R. D. Moffat, Phys. Rev. **96**, 374 (1954); α+O^{16}—J. R. Cameron, Phys. Rev. **90**, 839 (1953); and α+Ne—E. Goldberg *et al.*, Phys. Rev. **93**, 799 (1954).

[10] The argument to be presented will still hold if tails of other levels involving only even l's are included.

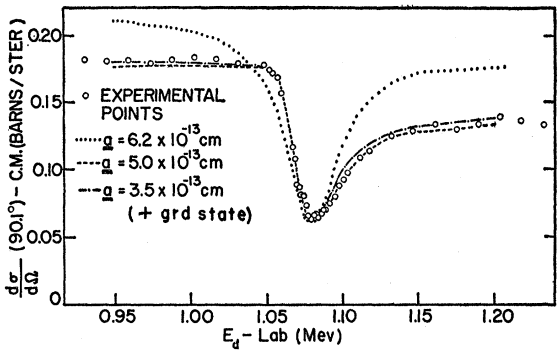

FIG. 2. Deuteron-helium scattering data over 1.07-Mev resonance at 90° (c.m.). Curves (dotted, dashed and dot-dashed) are theoretical fits to the data for different assumed interaction distances a. For $a=3.5\times10^{-13}$ cm sufficient ground-state resonant S-wave was added to the hard-sphere S-wave to make the resultant S-vector equal to that for hard-sphere alone with $a=5.0\times10^{-13}$ cm.

had not been present because $P_l=0$ at 90° for all odd l. While P'' also vanishes at 90° for all odd l, P_l' does not. Thus, $|C|^2$ and $|D|^2$ will not be zero and hence will contribute to the cross section on the resonance. But their contribution cannot interfere with the smooth contribution of $|A|^2$ and $|B|^2$—they can only add to the cross section. Hence, a dip (interference) in the 90° cross section means the resonance involves even l.[11]

Similar qualitative assignments can be extended to behavior at other angles for which various P_l vanish.

The Wigner limit on reduced widths, $\gamma_\lambda, l^2 \leqq \frac{3}{2}\hbar^2/\mu a$, likewise limits the l values which have to be considered since the penetrability, $1/A_l^2$, decreases monotonically with increasing l. Hence, for a given observed width, there exists a highest l consistent with the Wigner limit.

V. ANALYSIS OF THE DEUTERON-HELIUM CROSS SECTIONS

Although there is no *a priori* reason to assume the collision matrix is diagonal in l,[12] it was possible to fit the deuteron-helium cross sections by using only one l-value for each resonance. In this case $U_l^J=\exp(2i\delta_l^J)$, where $\delta_l^J=\phi_l+\beta_l^J$, and a simpler version[13] of Eq. (2) could be used for most of the calculations. The graphical method of analysis[14,15] in which the U_l^J are treated as vectors and circles in the complex plane has been used here.

A. 1.07-Mev Resonance

The open circles in Figs. 1 and 2 are experimental points taken from the preceding paper. The pronounced dip at 90° establishes the parity of the 1.07-Mev resonance as even. (See Sec. IV.) For $a=6.2\times10^{-13}$ cm, which is a generous estimate for the sum of the conventional deuteron and α-particle radii, the maximum width consistent with the Wigner limit for an $l=4$ resonance at 1.07 Mev is less than 1 kev, whereas the observed width is 35 kev. For smaller values of a the maximum width for $l=4$ is even less than 1 kev. Hence, the resonance must involve l-values less than 4. Because of the even parity only $l=0$ and $l=2$ need be considered.

The 1^+ circles for $l=0$, $l=2$, or any combination of 0 and 2 are much too small to produce the large peak observed at the back angle, 173.6°. The same is true for 2^+. In addition, a 2^+ resonance would produce a peak rather than a dip at 90°. The only remaining possible assignment is 3^+.

The back angle (173.6° c.m.) and 90° (c.m.) are the most convenient angles for extracting phase shifts because $\sin^2\theta$ is small (0.0123) at 173.6° and because at 90° $P_l=P_l''=0$ for odd l and $P_l'=0$ for even l.

Since D and higher angular momentum potential phase shifts are negligible, since there is no P-wave scattering at 90°, and since the level is certainly 3^+, the 90° data can be used to uniquely fix the S-wave phase shift and the resonance parameters γ_λ^2 and E_λ. When the S-wave phase shift and resonance parameters are fixed, then the back-angle data can be used to determine the P-wave phase shifts. The fit at intermediate angles (Fig. 2 of preceding paper) serves as a check on the total phase shift analysis.

When the above procedure was followed, the required P-wave phase shift had to be near zero or slightly positive in the neighborhood of the 1.07-Mev resonance. From Fig. 3 we see that P-wave hard-sphere phase shifts are *negative* and in magnitude from 2° to 10° for

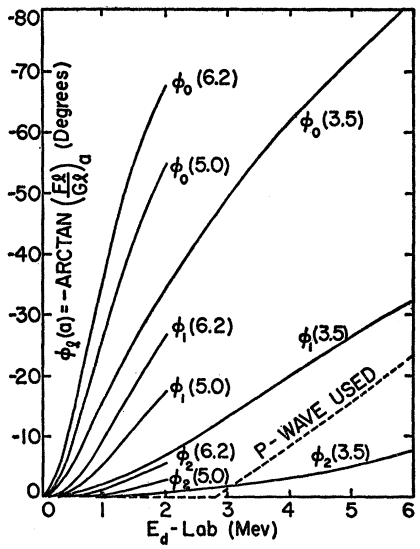

FIG. 3. S, P, and D hard-sphere phase shifts for different interaction distances a. Also, the P phase shift (dashed curve) used in the calculations of final theoretical fit to deuteron-helium scattering data.

[11] Not all even l resonances, however, have dips at 90°.

[12] When there is a large decrease in penetrability from l to $l+2$, the importance of the corresponding nondiagonal term will, of course, be greatly reduced.

[13] Lauritsen, Huus, and Nilsson, Phys. Rev. **92**, 1501 (1953).

[14] R. A. Laubenstein and M. J. W. Laubenstein, Phys. Rev. **84**, 18 (1951).

[15] H. L. Jackson and A. Galonsky, Phys. Rev. **84**, 410 (1951).

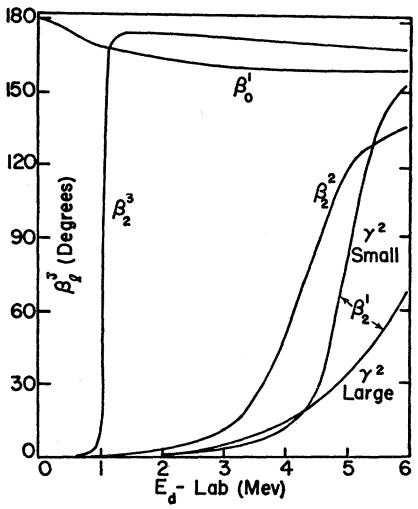

FIG. 4. The resonant phase shifts used in the final calculations of the theoretical fit to the data. "γ^2 small" and "γ^2 large" correspond to extreme assumptions for the size of the reduced width of the 1^+ level.

reasonable interaction radii (3 to 6×10^{-13} cm). It is, therefore, apparent[16] that the P-wave phase shift finally employed does not correspond to hard sphere scattering.

Corroborative evidence on the P-wave phase shift comes from a consideration of the ordering of the peak resonance cross section with angle. Since the 3^+ resonance is a D-resonance and $P_2(\cos125.2°)=0$, there is no interference between resonant and non-resonant scattering at 125.2°. Hence, the energy of the peak in the 125.2° data is the resonant energy, E_R, where $\beta_2^3=90°$. As the back angle peak occurs at slightly higher energy (3 ± 2 kev) than does the 125.2° peak (see Table II, preceding paper), β_2^3 must be $>90°$ at the back angle peak. With a negative P-wave phase shift, however, this peak would occur for $\beta_2^3<90°$. Thus the ordering with angle of the peak cross section actually requires a small positive P-wave phase shift; however, to simplify the calculations a zero P-wave was used. The significance of the anomalous P-wave phase shift will be discussed later.

The S-wave phase shift extracted from the 90° data does correspond to a hard sphere potential of radius approximately 5×10^{-13} cm. However, the same resultant S-wave phase shift can be produced by a combination of the S-wave tail from the bound[17] (ground) state of Li^6 and a smaller hard sphere radius. The ground state of Li^6 is known to be 1^+. The very small quadrupole moment[18] of Li^6 and the value of the magnetic moment of Li^6 suggest[19] that the ground state is almost pure S state.

A lower limit of $\sim3\times10^{-13}$ cm for the hard-sphere radius results from assuming a reduced width equal to the Wigner limit for the ground state of Li^6. Conversely, a very small reduced width of the ground state of Li^6 requires the large 5×10^{-13} cm hard-sphere radius.

Figure 2 illustrates this latitude in variation of the hard-sphere radius for which it is possible to compensate by adjusting the ground-state reduced width. It will be noted that the interaction distance a cannot be chosen appreciably larger than 5×10^{-13} cm nor less than $\sim3\times10^{-13}$ cm.[20] Figure 1 shows the similar situation at the back angle where P-wave potential phases should also contribute. The 30 percent or more discrepancy for $E_d>1.1$ Mev should be noted when hard-sphere P-wave phase shifts are employed. However, the excellent fit shown by the solid curves in Fig. 2, preceding paper, can be obtained at all angles if the P-wave phase shift is made zero or slightly positive. These curves were calculated for the resonant phase shifts shown in Fig. 4. The hard-sphere potential phase shifts, (Fig. 3) corresponding to $a=3.5\times10^{-13}$ cm were used except for the P-wave which was zero.

B. High-Energy Anomaly

The high-energy anomaly (Fig. 3, preceding paper) has a slight minimum around 4 Mev at 90°. The dashed curve in the figure was calculated from Rutherford and hard-sphere scattering and the tails of the ground and 3^+ states with $a=3.5\times10^{-13}$ cm, but no other level was assumed. It is seen that the effect of the level is to reduce the cross section from what it would have been in the absence of that level. This interference at 90° again can occur only for an even parity level.

Although the width (as measured from the back angle data) is much greater than that of the 1.07-Mev resonance, the energy, and thus the penetration are also much greater. The net result is that again the resonance must involve l-values less than 4, and because of the parity only $l=0$ and $l=2$ need be considered. In terms of J and parity, the possible choices are 1^+, 2^+, and 3^+.

However, the 1^+ circles are much too small to pro-

[16] $A-2°$ P-wave phase shift causes a 30 percent discrepancy in cross section at the back angle on the high side of the 1.07-Mev resonance. (See dot-dashed curve of Fig. 1.)

[17] The phase shifts resulting from a bound state are determined from the usual resonance formula once the constants γ_λ^2 and E_λ are fixed. [A useful approximate formula for g_l for negative energies is given by R. G. Thomas, Phys. Rev. 88, 1109 (1952).] The known binding energy of Li^6 against deuteron+α-particle breakup, 1.477 Mev, provides one condition on these constants. The second condition was obtained by requiring that the ground-state phase shift at 1.07 Mev be just right to make up the difference between the hard-sphere S-wave phase shift and that needed to fit the 90° data. When $a=3.5\times10^{-13}$ cm, the parameters resulting from these two conditions are $\gamma_\lambda^2=6.85\times10^{-13}$ Mev-cm (c.m.) and $E_\lambda=-5.62$ Mev (lab). The energy dependence of the ground state phase shift, β_0^1, calculated with the above parameters, is illustrated in Fig. 4.

[18] N. A. Schuster and G. E. Pake, Phys. Rev. **81**, 157 (1951).

[19] J. M. Blatt and V. F. Weisskopf, *Theoretical Nuclear Physics* (J. Wiley and Sons, New York, 1952), p. 251, Table 5.1.

[20] It is also interesting that the lower permissible interaction radius (3×10^{-13} cm) corresponds very closely to the sum of the directly measured radii of the deuteron ($1.5\pm0.2\times10^{-13}$ cm) and the alpha particle ($1.4\pm0.2\times10^{-13}$ cm). The measurements are by McIntyre and Hofstadter and by Hofstadter, McAllister, and Wiener, Phys. Rev. **96**, 854(A) (1954).

duce the observed back-angle peak cross section at 4.62 Mev.

The 2^+ and 3^+ circles are big enough for the back-angle peak if some flexibility is given to the choice of P-wave. Since the P-wave does not enter at 90°, this is an excellent testing angle for 2^+ and 3^+. The dotted and dot-dashed curves (Fig. 3, preceding paper), however, show that neither 2^+ nor 3^+ will fit the data. It must be concluded that no single level can account for these cross sections.

In the absence of higher energy data one would not conclude from *looking* at the cross-section curves that there is more than one level present. However, if further attempts are to be made to fit the data, the next simplest assumption is that two levels are involved. At least one level must be broad and, therefore, excited by $l \leqq 2$. The other level cannot be very sharp because it would then have been seen as a separate resonance. The single-level possibilities considered above gave a poor fit to the data over an energy range of at least 0.5 Mev. Thus any additional level brought in must be capable of influencing the cross section over at least 0.5 Mev extent. As the width of an $l=3$ resonance at 4 Mev must be less than 100 kev, there is certainly no loss of generality in requiring that $l<4$ for both resonances.

With this restriction there are 36 possible two-level combinations. Most of them can be ruled out very easily. The 36 combinations are presented in the array in Fig. 5. Each row and each column are labelled with a J and parity. The box in the 3^+ row and 2^+ column has the statement "too high at back angle." This means that the combination $(3^+, 2^+)$ produces much too high a cross section at the back angle. The other statements have similar meanings. The 14 combinations of

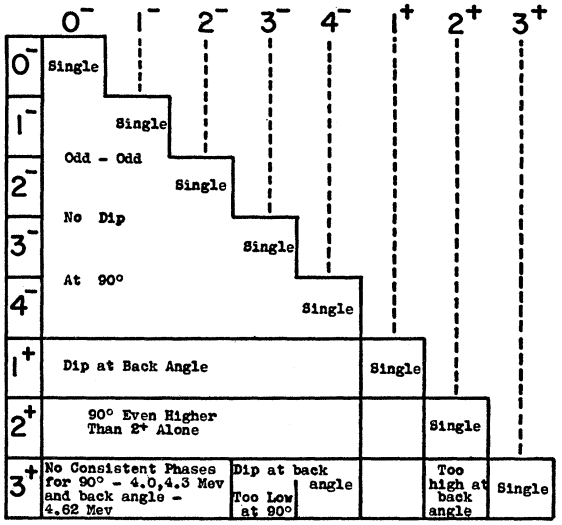

FIG. 5. Array of 36 two-level combinations possible for the high-energy anomaly ($l<4$ for excitation of both levels) with arguments against 34 of them. The combination $(3^+, 1^+)$ was eliminated by detailed calculation. Only $(2^+, 1^+)$ fitted the data.

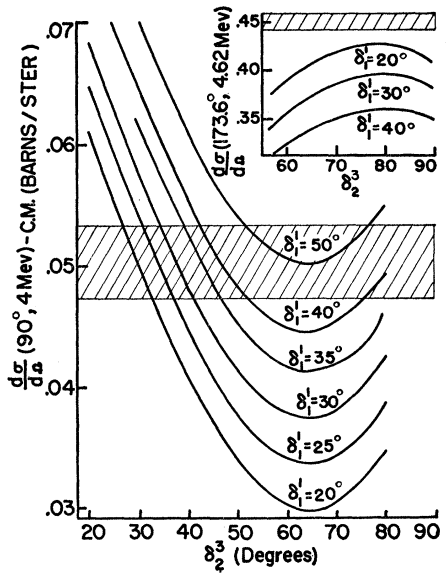

FIG. 6. Calculated cross sections at 90° (c.m.) for the possible combination $(3^+, 1^-)$ for the high-energy anomaly. ($\delta_l{}^J = \beta_l{}^J + \phi_l$.) Curves are calculated for a given $\delta_1{}^1$ as a function of $\delta_2{}^3$. Cross-hatched area corresponds to range of cross sections allowed by experimental measurement plus limits of errors at 4.0 Mev. Inset is a similar set of calculated curves and measurement range for 4.62 Mev at 173.6° (c.m.).

two odd parity levels are all ruled out by the same reason—that they cannot produce a dip at 90°. The word "Single" appears in the diagonal elements of the array where the two levels have the same J and parity. These combinations are forbidden for the same reason as a single level of the same J and parity, i.e., the maximum contribution for a given partial wave occurs for a given phase shift, $\delta_l{}^J$, independent of whether that phase shift is produced by one or a dozen levels. In the case of n levels of the same J and parity the resonant phase shifts merely traverse all phase angles n times. Of the other statements only that for 3^+ with 0^-, 1^-, and 2^- requires explanation. For illustration $(3^+, 1^-)$ will be discussed in some detail. The arguments against $(3^+, 0^-)$ and $(3^+, 2^-)$ are similar.

Each curve in Fig. 6 gives the calculated cross section at 90°, 4 Mev as a function of the 3^+ phase shift, $\delta_2{}^3$, for a particular value of the 1^- phase shift, $\delta_1{}^1$. The experimental cross section is 0.050 barn/sterad, with an uncertainty indicated by the cross-hatching. The insert gives the same information for the back angle at 4.62 Mev. The insert also shows that $\delta_1{}^1 < 20°$ at 4.62 Mev, with $\delta_2{}^3 \approx 80°$. These phase shifts must be smaller at 4 Mev, but it will be assumed that the 1^- resonance is so broad that $\delta_1{}^1$ is constant at 20° all the way from 4 to 4.62 Mev. Although this is certainly impossible and even weakens the argument, it does make it easier to follow. For small $\delta_1{}^1$ to fit the 90° cross section, $\delta_2{}^3$ must be $\sim 30°$ at 4 Mev. The Rutherford and "potential" vectors change so little from 4 to 4.3 Mev that except for the change in the factor $(1/k^2)$,

the calculated curves for 4.3 Mev at 90° are essentially the same as those in Fig. 6 for 4 Mev at 90°. The change in $(1/k^2)$ shifts the curves down by $7\frac{1}{2}$ percent. Hence, if the extreme value of $\delta_1{}^1=20°$ is assumed then $\delta_2{}^3$ must vary from 30° at 4 Mev to 80° at 4.62 Mev, and the 90° cross section then follows the $\delta_1{}^1=20°$ curve from 4 Mev ($\delta_2{}^3=30°$) to 4.62 Mev ($\delta_2{}^3=80°$). Such phase shifts imply a deep minimum in the 90° cross section beyond 4 Mev, whereas the data (Fig. 3, preceding paper) indicate a slight rise. Thus at 4.3 Mev $\delta_2{}^3$ would be $\approx 60°$ and hence $d\sigma/d\Omega(90°)=0.030-7\frac{1}{2}$ percent, which is only half the experimental value. A more realistic choice of phase shifts would have made this discrepancy even greater. Thus, while 3^+ and 1^- phase shifts can be chosen to fit the 90° data at 4 Mev and the back-angle data at 4.62 Mev, there is no set of phases consistent with the required energy dependence that will fit the 90° data beyond 4 Mev.

Investigation of the combination $(3^+, 1^+)$ was complicated by the possibility of both S-wave and D-wave excitation of the 1^+ level, making a qualitative or semi-quantitative analysis indecisive. Detailed calculations have shown, however, that all of the data cannot be fitted by $(3^+, 1^+)$. Since the 1.07-Mev resonance is also 3^+, it was necessary to use a two-level formula in calculating the 3^+ phase shifts. This formula is included for reference[21]:

$$\tan\beta_l{}^J=\frac{k/A_l{}^2}{\left(\dfrac{\gamma_{\lambda 1}{}^2}{E_{\lambda 1}-E}+\dfrac{\gamma_{\lambda 2}{}^2}{E_{\lambda 2}-E}\right)^{-1}-\dfrac{1}{a}(g_l+l)}.$$

Of course, one would not expect two broad levels of the same J and parity so close together (2.2 and 4.5 Mev excitation in Li^6).

With the one remaining two-level combination, $(2^+, 1^+)$, there was no difficulty in obtaining a fit to the data. The solid curves in Fig. 3, preceding paper, were calculated for the resonant phase shifts shown in Fig. 4. The hard sphere potential phase shifts (Fig. 3) corresponding to $a=3.5\times10^{-13}$ cm were used except for the P-wave, which was modified as indicated by the dashed curve in Fig. 3.

In Fig. 4 it will be noted that $\beta_0{}^1$ and $\beta_2{}^3$ do not increase monotonically with energy as is ordinarily expected for a resonant phase shift. However, if one recalls that $\tan\beta_l{}^J=k\gamma_{\lambda,\,l}{}^2/[(E_R-E)A_l{}^2]$, then it is apparent that under certain conditions the penetration factor, $A_l{}^{-2}$, may increase faster with energy than E_R-E. Thus, $\beta_l{}^J$ may recede from 180° for a while as the energy increases beyond the resonant energy. Eventually for large E, $A_l{}^{-2}\rightarrow$ constant and, hence, $\beta_l{}^J\rightarrow 180°$.

TABLE I. Li^6 level parameters determined for $a=3.5\times10^{-13}$ cm.

(J,π,T)	$\gamma^2/\frac{3}{2}\frac{\hbar^2}{\mu a}$	Excitation in Li^6 E_x (Mev)	E_λ (Mev)
(1, +, 0)	0.51	0	−2.26
(3, +, 0)	0.80	2.185±0.003	2.333
(2, +, 0)	1.0	4.52 ±0.08	7.05
(1, +, 0)	0.2−1.0	4.9 −5.8	5.5−9.7

[21] R. K. Adair (private communication).

The level parameters corresponding to the resonant phase shifts of Fig. 4 are displayed in Table I. Here, as for the lower energy data, the parameters were determined from the 90° and back angle data only. The P-wave was at first taken to be zero and then adjusted to the values in Fig. 4 in order to improve the fit at 125.2° where $P_2(\cos\theta)=0$. Excitation of the 1^+ level was assumed to be entirely by D-waves. The possibility of some S-wave excitation was not examined except for the case of 100 percent S-wave and no D-wave, and this case gives too low a peak at the back angle.

Although the calculated curves are somewhat outside of the experimental uncertainties at some energies and angles, there are quite a few parameters whose variation might improve the general agreement. In particular, the tendency for some of the curves to fall too low might be rectified by the use of a larger interaction distance. This would increase the D-wave penetrability and, thus, allow larger 2^+ and 1^+ phase shifts. At 3 and 3.5 Mev an additional 1.8° of $\delta_2{}^2$ would remove the discrepancy at the back angle.

Only the beginning of the 1^+ resonance can be seen at the deuteron bombarding energies available in this experiment. At 4.3 Mev, which was the highest energy for all angles but the back angle, $\beta_2{}^1$ is only 18.4°. Although the level assignment made on the basis of the tail of the resonance is believed reliable, there is great latitude in the choice of $\gamma_\lambda{}^2$ and E_λ. The phase shifts produced by the two extreme values of $\gamma_\lambda{}^2$ are given in Fig. 4. The value of E_λ, for a given reduced width was determined by the requirement that the phase shift at 4.3 Mev be 18.4°. The cross sections at 90°, 125.2°, and 173.6° have been calculated up to 6 Mev for the two limiting sets of parameters and are indicated by the two solid curves for each of these angles in Fig. 3, preceding paper. If the assumption of no S-wave excitation of the 1^+ level is true, and if there are no additional levels up to 6 Mev, then the experimental points should lie between the two sets of curves.

VI. COMPARISON WITH OTHER WORK

The assignment 3^+ to the $E_d=1.07$-Mev resonance confirms the work of Lauritsen, Huus, and Nilsson.[13] Their 3^+ assignment was based on $He^4(d,d)He^4$ differential cross section measurements at 90°, 120°, and 156° c.m. from 1.0 to 1.2 Mev. For the resonant energy they obtained $E_R=1.070\pm0.002$ Mev, which agrees with our value here. All of the curves they calculated at their back angle (156° c.m.) were too low around 1.2 Mev. Since they used hard-sphere P-wave phase shifts,

the discrepancy is corroborative evidence against using negative P-wave phase shifts in this energy region.

After our phase-shift analysis was completed, we learned of recent unpublished work of Allen, Almquist, and Bigham[22] who have investigated the levels of Li^6 and He^6 by means of reactions $Li^7(He^3,\alpha)Li^6$ and $Li^7(t,\alpha)He^6$. Comparison of levels in He^6 and Li^6 permit assigning isobaric spin $T=1$ to the levels of Li^6 which they observe at 3.56 ± 0.06, 5.31 ± 0.07, and 6.63 ± 0.08-Mev excitation. In addition they see levels in Li^6 at 2.2, 4.30 ± 0.2, ~5.5 Mev, and 7.40 ± 0.08 Mev which they believe to be $T=0$ levels. It is only these latter levels ($T=0$) which can influence the deuteron alpha scattering if isobaric spin is a good quantum number. Their levels at 2.2, 4.30 ± 0.2, and 5.5 Mev in general agree within the assigned uncertainties with the levels obtained from the present phase-shift analysis at 2.185 ± 0.003, 4.52 ± 0.08, and 5.3 ± 0.5-Mev excitation.

VII. CONCLUSIONS

1. Anomalous P-Wave

The large departure of the empirically adjusted P-wave phase from that calculated on hard-sphere scattering may most simply be interpreted in terms of positive phase shifts from one or more P-wave resonances which lie beyond the presently investigated energy range. Such low-lying odd-parity levels could not arise from the usually assumed $(p)^2$ configuration of the independent-particle model. However, as Wigner[23] has so strongly emphasized, the symmetry properties of the nuclear wave functions for interchange of particles require that configurations which give the strongest binding also give the strongest repulsion. Hence the splitting between the high and low terms of the $(p)^2$ configuration is expected to be very great (contrasted to the atomic case). Therefore, it should not be surprising that the low space-symmetric terms of the (s,p) or (d,p) configurations will overlap the higher terms of the $(p)^2$ configuration. Higher-energy scattering data are, however, needed to locate and characterize the states producing the anomalous P-wave phase shifts here observed.

2. Reduced Widths

The reduced width measures the overlap of the internal wave function of the compound nucleus, Li^6, with the deuteron+alpha wave function at the nuclear surface. If, in a certain state of Li^6, the two wave functions are identical, then the overlap is complete and the reduced width has its maximum value. Such a state is called a single-particle state, the single particles being in this case the deuteron and the alpha particle.

All three of the levels observed in this experiment have reduced widths of the same order of magnitude as $\frac{3}{2}\hbar^2/\mu a$, suggesting a high degree of pure single-particleness in the wave functions for these three states. It is not possible to measure γ^2 very accurately because only the product of γ^2 and the penetrability is directly observed. The penetrability is a sensitive function of the interaction distance, which was not too well fixed by this experiment.

The parameters listed in Table I are those used for the solid curves in Figs. 2 and 3, preceding paper. The interaction distance was $a=3.5\times10^{-13}$ cm. If $a=5.0\times10^{-13}$ cm had been used, the values of $\gamma^2/(\frac{3}{2}\hbar^2/\mu a)$ would have been about half as big as those listed, the values of E_λ somewhat smaller, but the E_R, of course, would be unchanged.

3. Li^6 Levels and Intermediate Coupling

All of the known levels of Li^6 are plotted in the two central columns of Fig. 7. The 3^+, 2^+, and 1^+, $T=0$ levels are the levels investigated in this experiment. The deuteron bombarding energy corresponding to 3.58-Mev excitation in Li^6 is 3.15 Mev. Figure 1, preceding paper, shows no sign of a resonance at this energy even though the energy steps were 3 kev. This absence of a resonance is consistent with the assignment 0^+, $T=1$. The $T=1$ levels at 5.31 ± 0.07 and 6.63 ± 0.08 Mev and the 7.40 ± 0.08 Mev $T=0$ level have been observed by Allen *et al.* at Liverpool.[22]

The left- and right-hand columns of Fig. 7 contain the levels predicted by Inglis[24,25] with a rather simple intermediate coupling calculation on the two p-shell nucleons in Li^6.

Since only the 3^+, $T=0$ and 0^+, $T=1$ levels were used in fixing the constants, a comparison between

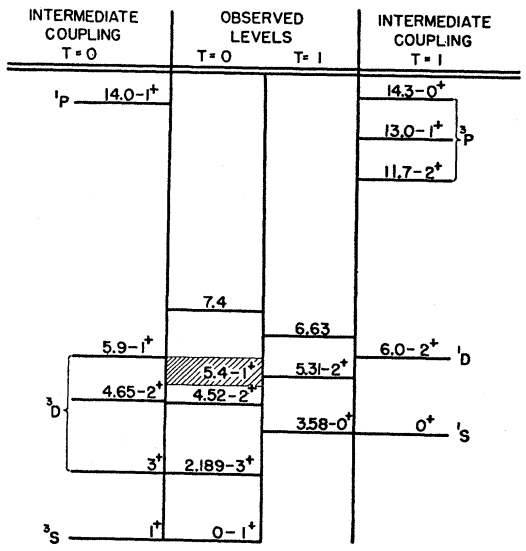

FIG. 7. Central two columns are experimental observations of this and other experiments. Columns labeled "Intermediate coupling" are from calculations of Inglis (see references 24 and 25) with an intermediate coupling model near the $L-S$ extreme.

[22] K. W. Allen (private communication).
[23] E. Wigner, Phys. Rev. **51**, 947 (1937).
[24] D. R. Inglis, Phys. Rev. **87**, 915 (1952).
[25] D. R. Inglis, Revs. Modern Phys. **25**, 390 (1953).

theory and experiment can be made with the other observed levels. The rather satisfactory agreement found for the lowest levels lends support to an intermediate coupling model rather near the pure $L-S$ extreme. The presence of a $T=1$ level at 6.63 and a $T=0$ level at 7.40 Mev as reported by Allen, *et al.*, however, cannot be accounted for in terms of the $(p)^2$ configuration. These levels may belong to the higher configurations postulated in Sec. IV to account for the anomalous P-wave phase shift.

4. Li^6 Levels and the Tensor Force

A major deficiency of the intermediate coupling method is that it provides no understanding of the origin of the spin-orbit force. A more fundamental approach has been made by Feingold,[26] who calculated the splitting in $L-S$ coupling between the ground state and the 0^+, $T=1$ state by the tensor force, a force which is already necessary to explain the quadrupole moment of the deuteron. Although the splitting is in the right direction, the magnitude is only half the observed value.

More extensive calculations of the tensor force splitting in Li^6 have recently been made by Lyons.[27] These calculations include the splitting of the four D levels as well as the two S levels. The agreement with experiment is again only qualitative.

VIII. ACKNOWLEDGMENTS

The authors are grateful to W. Haeberli and H. T. Richards for enlightening discussions on the analysis of the scattering data and on the interpretation of the Li^6 levels.

APPENDIX I

A general partial wave expansion of the differential cross section is given by Sachs[28]:

$$\left(\frac{d\sigma}{d\Omega}\right)_{\sigma\sigma'}=\frac{\pi}{k_\sigma^2}\left|\sum_{l,l'} i^{(l-l')}(2l+1)^{\frac{1}{2}} \times e^{\frac{1}{2}i(\alpha_l+\alpha_{l'})}(U-1)_{ss'}Y_{l'}^{m'}(\sigma')+\frac{iR_\sigma}{\sqrt{\pi}}\delta_{\sigma\sigma'}\right|^2. \quad (1)$$

The notation has been changed slightly to agree with that used in previous analyses. Sachs uses η_l and ρ_σ instead of α_l and R_σ. These quantities are simply related as follows:

$$\alpha_l=2(\eta_l-\eta_0)$$

$$R_\sigma=\pi^{\frac{1}{2}}e^{-2i\eta_0}\rho_\sigma.$$

[26] A. M. Feingold, Ph.D. thesis, Princeton University, 1952 (unpublished).
[27] A. M. Feingold (to be published).
[28] See reference 5, p. 287. A factor i was inadvertently omitted from the Rutherford term in Sachs' equation (10–11).

The quantities appearing in (1) are defined as follows: $(d\sigma/d\Omega)_{\sigma\sigma'}$ = differential cross section per unit solid angle in the center-of-mass system for incident and outgoing particles whose identities and spin orientations are denoted by σ and σ'. k_σ = wave number of relative motion for incident waves $=\mu v/\hbar$, where μ is the reduced mass and v is the relative velocity of the two particles. l = quantum number of the wave of orbital angular momentum $l\hbar$. α_l = Coulomb phase shift $=2$ arctan$(\eta+\eta/2+\cdots+\eta/l)$ except that $\alpha_0=0$. $\eta=zz'e^2/\hbar v$, where z and z' are the atomic numbers of the two particles. (η is not one of Sach's η_l.) U = collision matrix. $Y_{l'}^{m'}(\sigma')$ = spherical harmonic of the outgoing wave. It is given by

$$Y_{l'}^{m'}(\sigma)=(-1)^{\frac{1}{2}(m'+|m'|)}\left[\frac{2l'+1}{4\pi}\frac{(l'-|m'|)!}{(l'+|m'|)!}\right]^{\frac{1}{2}} \times\sin^{|m'|}\theta e^{im'\varphi}\frac{d^{|m'|}P_{l'}(\cos\theta)}{d(\cos\theta)^{|m'|}},$$

where

$$P_l(x)=\frac{1}{2^l l!}\frac{d^l(x^2-1)^l}{dx^l},$$

and θ and φ are the center-of-mass polar and azimuthal angles of observation with respect to the incident beam direction. R_σ = Rutherford amplitude of the incident wave $=-\frac{1}{2}\eta\csc^2(\theta/2)\exp[i\eta\ln\cos^2(\theta/2)]$. $\delta_{\sigma\sigma'}$ = Kronecker delta. s denotes l and m as well as σ.

As given in (1), the U-matrix is in an (S,l,m_S,m_l) representation. Transforming to an (S,l,J,m_J) representation with the aid of the Clebesch-Gordan coefficients[29] and specializing to the case of elastic scattering of spin 1 with spin 0 particles, we find from Eq. (1) the partial cross sections, $(d\sigma/d\omega)m_S$, $m_{S'}$, where m_S and $m_{S'}$ give the incident and scattered spin orientations with respect to the incident beam axis:

$$k^2\left(\frac{d\sigma}{d\Omega}\right)_{+1,+1}=k^2\left(\frac{d\sigma}{d\Omega}\right)_{-1,-1}=|A|^2,$$

$$k^2\left(\frac{d\sigma}{d\Omega}\right)_{0,0}=|B|^2,$$

$$\frac{k^2}{\sin^2\theta}\left(\frac{d\sigma}{d\Omega}\right)_{+1,0}=\frac{k^2}{\sin^2\theta}\left(\frac{d\sigma}{d\Omega}\right)_{-1,0}=\frac{|C|^2}{2},$$

$$\frac{k^2}{\sin^2\theta}\left(\frac{d\sigma}{d\Omega}\right)_{0,+1}=\frac{k^2}{\sin^2\theta}\left(\frac{d\sigma}{d\Omega}\right)_{0,-1}=\frac{|D|^2}{2},$$

$$\frac{k^2}{\sin^4\theta}\left(\frac{d\sigma}{d\Omega}\right)_{+1,-1}=\frac{k^2}{\sin^4\theta}\left(\frac{d\sigma}{d\Omega}\right)_{-1,+1}=\frac{|E|^2}{2}.$$

[29] E. U. Condon and G. H. Shortley, *The Theory of Atomic Spectra* (Cambridge University Press, London, 1951), p. 76.

In the usual case, where the beam is unpolarized and the three possible values of $m_{S'}$ are indistinguishable, a sum over $m_{S'}=0,\pm1$ for each m_S and then an average over $m_S=0,\pm1$ is performed. The result is:

$$3k^2\frac{d\sigma}{d\Omega}=2|A|^2+|B|^2+\sin^2\theta\{|C|^2+|D|^2\}+\sin^4\theta\{|E|^2\},$$

where

$$A=R+\sum_l\frac{e^{\frac{1}{2}i\alpha_l}}{4i}\{e^{\frac{1}{2}i\alpha_l}P_l[(l+2)U_{ll}{}^{l+1}+(2l+1)U_{ll}{}^{l}+(l-1)U_{ll}{}^{l-1}-2(2l+1)]-e^{\frac{1}{2}i\alpha_{l+2}}P_{l+2}\times[(l+1)(l+2)]^{\frac{1}{2}}U_{l,l+2}{}^{l+1}-e^{\frac{1}{2}i\alpha_{l-2}}P_{l-2}\times[l(l-1)]^{\frac{1}{2}}U_{l,l-2}{}^{l-1}\},$$

$$B=R+\sum_l\frac{e^{\frac{1}{2}i\alpha_l}}{2i}\{e^{\frac{1}{2}i\alpha_l}P_l[(l+1)U_{ll}{}^{l+1}+lU_{ll}{}^{l-1}-(2l+1)]+e^{\frac{1}{2}i\alpha_{l+2}}P_{l+2}[(l+1)(l+2)]^{\frac{1}{2}}U_{l,l+2}{}^{l+1}+e^{\frac{1}{2}i\alpha_{l-2}}P_{l-2}[l(l-1)]^{\frac{1}{2}}U_{l,l-2}{}^{l-1}\},$$

$$C=\sum_l\frac{e^{\frac{1}{2}i\alpha_l}}{2i}\left\{\frac{e^{\frac{1}{2}i\alpha_l}P_l'}{l(l+1)}[l(l+2)U_{l,l}{}^{l+1}-(2l+1)U_{ll}{}^{l}-(l^2-1)U_{ll}{}^{l-1}]+e^{\frac{1}{2}i\alpha_{l+2}}P_{l+2}{}'\left[\frac{(l+1)}{(l+2)}\right]^{\frac{1}{2}}U_{l,l+2}{}^{l+1}-e^{\frac{1}{2}i\alpha_{l-2}}P_{l-2}{}'\left(\frac{l}{l-1}\right)^{\frac{1}{2}}U_{l,l-2}{}^{l-1}\right\},$$

$$D=\sum_l\frac{e^{\frac{1}{2}i\alpha_l}}{2i}\left\{e^{\frac{1}{2}i\alpha_l}P_l'[U_{ll}{}^{l+1}-U_{ll}{}^{l-1}]-e^{\frac{1}{2}i\alpha_{l+2}}P_{l+2}{}'\times\left[\frac{(l+1)}{(l+2)}\right]^{\frac{1}{2}}U_{l,l+2}{}^{l+1}+e^{\frac{1}{2}i\alpha_{l-2}}P_{l-2}{}'\left(\frac{l}{l-1}\right)^{\frac{1}{2}}U_{l,l-2}{}^{l-1}\right\},$$

$$E=\sum_l\frac{e^{\frac{1}{2}i\alpha_l}}{2\sqrt{2}i}\left\{\frac{e^{\frac{1}{2}i\alpha_l}P_l''}{l(l+1)}[lU_{ll}{}^{l+1}-(2l+1)U_{ll}{}^{l}+(l+1)U_{ll}{}^{l-1}]-\frac{e^{\frac{1}{2}i\alpha_{l+2}}P_{l+2}{}''}{[(l+1)(l+2)]^{\frac{1}{2}}}U_{l,l+2}{}^{l+1}-\frac{e^{\frac{1}{2}i\alpha_{l-2}}P_{l-2}{}''}{[l(l-1)]^{\frac{1}{2}}}U_{l,l-2}{}^{l-1}\right\}$$

PHYSICAL REVIEW VOLUME 98, NUMBER 3 MAY 1, 1955

Gamma Radiation from Polonium Neutron Sources

R. J. Breen* and M. R. Hertz†
Mound Laboratory‡, Monsanto Chemical Company, Miamisburg, Ohio
(Received December 2, 1954)

A NaI(Tl) crystal scintillation spectrometer was used to investigate the gamma spectrum from Po-alpha bombardment of Li, Be, B, F, Na, Mg, and Al. The principal gamma energies observed were: Li, 0.483 Mev; Be, 4.45 Mev; B, 2.36 and 3.68 Mev; F, 1.28 and 1.51 Mev; Na, 1.83 and 2.57 Mev; Mg, 1.30, 1.82, and 2.97 Mev; Al, 1.25, 2.28, and 3.55 Mev. The probable origin of the gammas is discussed.

INTRODUCTION

PRIOR to discovery of the neutron, gamma radiation had been observed as a result of the action of alpha particles on some light nuclei.[1,2] Subsequent investigation established the existence of gamma radiation, in addition to neutron emission, from the bombardment of Li, Be, B, F, Na, Mg, and Al by alpha particles.[3]

During preparation of neutron sources by mixture of Po^{210} with various target materials, gamma radiation was observed in addition to that expected from the Po. An investigation of the energy and origin of this radiation would be of assistance in studies of neutron spectra and of efficiency of neutron production by polonium neutron sources.

An investigation of the gamma spectrum from polonium neutron sources was conducted with a NaI(Tl) single-crystal scintillation spectrometer. Data are presented for Po-Li, Po-Be, Po-B, Po-CaF_2, Po-Na, Po-Mg, and Po-Al neutron sources.

EXPERIMENTAL PROCEDURE

The detecting portion of the spectrometer consists of a Harshaw-mounted NaI(Tl) crystal 1.5 inches in diameter by 1 inch thick, coupled through a Lucite light-pipe to an RCA 5819 photomultiplier tube. Pulses from the phototube are amplified by an Atomic Instrument Company Model 205-B preamplifier and a Model 204-B linear amplifier, with an added input delay line for pulse shaping. The high-level output of the linear amplifier is coupled to an Atomic Instrument Company

* Present address: College of St. Thomas, St. Paul, Minnesota,
† Present address: Goodyear Atomic Corporation, Portsmouth. Ohio.
‡ Mound Laboratory is operated by Monsanto Chemical Company for the U. S. Atomic Energy Commission.
[1] W. Bothe and H. Becker, Z. Physik **66**, 289 (1930).
[2] H. C. Webster, Proc. Roy. Soc. (London) **A136**, 428 (1932).
[3] H. Slätis, Arkiv Mat. Astron. Fysik **35A**, No. 31, 1 (1948).